Structural dependence of terahertz radiation from multiferroic $BiFeO_3$ thin films

D. S. Rana,* K. Takahashi, K. R. Mavani, I. Kawayama, H. Murakami, and M. Tonouchi†
Institute of Laser Engineering, Osaka University, 2-6 Yamadaoka, Suita, Osaka 565-0871, Japan
(Received 8 June 2007; revised manuscript received 29 August 2007; published 14 January 2008)

We have investigated the structural dependence of terahertz-radiation emission from the multiferroic $BiFeO_3$ thin films on $(LaAlO_3)_{0.3}(Sr_2AlTaO_6)_{0.7}$ (0 0 1) substrate. The coherently strained films with thickness (t) $\leqslant 75$ nm relax partially to bulklike rhombohedral phase at $t \geqslant 110$ nm via a coexistence of these two phases in the thickness 80 nm $\leqslant t \leqslant 110$ nm. The strained films ($t \leqslant 75$) and the relaxed films ($t \geqslant 110$ nm) exhibit similar terahertz-emission efficiency in the absence of electric-field bias, and this efficiency increases for the intermediate thickness films having coexisting phases. These data combined with the electric-field (E) dependence of the terahertz-emission amplitude (E_{THz}) depict that the terahertz-emission efficiency in zero bias is nearly independent of the lattice, while the ferroelectric properties (revealed by E_{THz}-E hysteresis loops) are characteristics of both the lattice and the leakage current.

DOI: 10.1103/PhysRevB.77.024105 PACS number(s): 78.20.−e

The emission of terahertz radiation from strongly correlated electron oxide systems (SCES) reflects the dynamics of photogenerated carriers excited by ultrafast femtosecond laser pulses. Various intriguing features in terahertz radiation at the magnetic-, charge-, and spin-ordering temperatures of SCES and the use of terahertz emission in imaging and time-domain spectroscopy demonstrate the versatility of terahertz emission in exploring the physical properties of such systems.[1,2] After the high temperature superconductors and the charge-ordered manganites were examined by terahertz-radiation emission,[2] a recent discovery of terahertz-radiation emission from the room-temperature multiferroic $BiFeO_3$ perovskite system (see Refs. 3 and 4 for a review on multiferroics) is interesting in several ways, namely, (i) the emission takes place upon ultrafast modulation of the spontaneous polarization in thin films, (ii) terahertz radiation can be emitted from electrically poled films even in the absence of applied bias, and (iii) terahertz-emission amplitude as a function of electric field generates a hysteresis loop which is similar to the ferroelectric hysteresis loop.[5–7] Thus, this optical technique proves to be a promising probe for studying the ferroelectric properties, for imaging of the ferroelectric domains, and for providing a nondestructive readout method[5] for the data stored in an electrically polarized state of $BiFeO_3$.

Recently, we have successfully deposited phase-pure fully strained and relaxed $BiFeO_3$ (BFO) films on $(LaAlO_3)_{0.3}(Sr_2AlTaO_6)_{0.7}$ (0 0 1) (LSAT) substrate,[8] where the lattice misfit between BFO and LSAT is as large as 2.6%. A considerably weak but a systematic enhancement in magnetic moment (up to $\sim 0.1 \mu_B$/f.u.) was found to be associated with the strained lattice of BFO/LSAT films, while the relaxed lattice showed a bulklike magnetic moment.[8] This makes it imperative to explore the technologically more promising aspects of these films such as ferroelectric and terahertz-emission properties, and their dependence on the lattice. In the present work, we have investigated the thickness and/or structural dependence of the terahertz emission from the BFO/LSAT films, which is a crucial factor for elucidating the strain induced effects. We show that the terahertz-emission efficiency in the absence of applied bias is more related to the quality of films than to the lattice, while the terahertz emission as a function of electric field (which reflects ferroelectric properties) is dependent both on the lattice and the quality of films.

$BiFeO_3$ films with thicknesses of 65–200 nm were prepared using pulsed laser deposition (KrF excimer laser) of a bismuth-rich $Bi_{1.1}FeO_3$ target, as described elsewhere.[8] The various thin films used for terahertz-emission studies are 65 nm film (abbreviated as "film-A"), 75 nm film (film-B), 90 nm film (film-C), 95 nm film (film-D), 110 nm films annealed in O_2 pressures of 40, 10, and 2 kPa (respectively, film-E, film-F, and film-G), and 200 nm film (film-H). These BFO/LSAT thin films grow in (i) fully strained pseudomorphic tetragonal phase for film thickness (t) $\leqslant 75$ nm; (ii) the films with $t \geqslant 110$ nm grow from partially to fully relaxed bulklike rhombohedral phase; and (iii) films with 80 nm $\leqslant t \leqslant 110$ nm possess both the fully strained and partially relaxed phases.[8] Also, the increasing postdeposition O_2 annealing of 110 nm films results in the evolution of a strained phase, while the same does not have any impact on structure in 65 and 200 nm thin films. Amongst the 110 nm films, film-G is assumed as deposited 110 nm film because it is annealed in a low O_2 pressure of 2 kPa that does not result in the coexistence of two structural phases. We have already shown that the structural lattice of the coherently strained BFO/LSAT films (with c axis of 4.128 Å) is largely different from the relaxed lattice of the BFO/LSAT films and the coherently strained lattice of BFO/STO films (c axis of 4.02 Å), and, hence, is an ideal case for studying the effects of epitaxial strain.[8]

A standard terahertz-emission experimental setup as described in detail in Ref. 5 was used for detecting the terahertz radiation from BFO films. A dipole-type optical switch with a gap of 10 μm was fabricated on BFO thin films, while LT-GaAs with bow-tie configuration was used as detector. A mode-locked Ti:sapphire laser beam with a wavelength of 800 nm was split into pump and probe pulses. The pump pulses were passed through the $Ba_2B_2O_4$ single crystal for second harmonic generation (SHG) with a wavelength of 400 nm. These SHG laser pulses with a power of 10.8 mW were focused on the dipole-type optical switch of the BFO

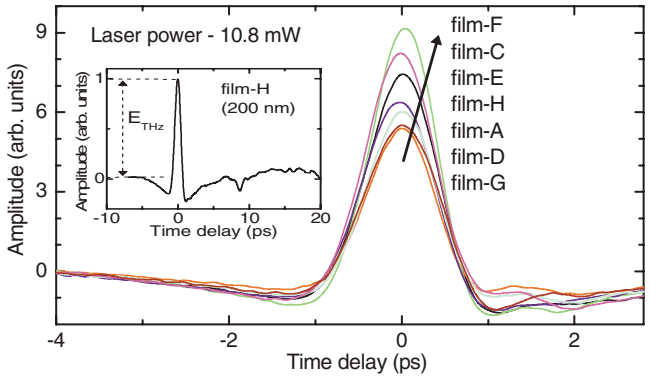

FIG. 1. (Color online) (a) Peak amplitude (E_{THz}) of the time-domain wave form in zero-bias electric field obtained after poling in +200 kV/cm for various thin films. The inset figure shows a typical terahertz time-domain wave form.

emitter. The LT-GaAs detector was illuminated by 800 nm laser pulses with a power of 10 mW. In order to authenticate the comparison of terahertz-emission amplitude of all the films, the entire optical path was fixed and only the sample was replaced each time at a fixed position. Most importantly, the same size of laser spot ~15 μm was used for illumination of optical switch of all the films.

Figure 1 shows the terahertz time-domain wave forms around the peak amplitude for all the BFO/LSAT thin films. The inset figure shows a typical time-domain wave form and the method for determination of the peak terahertz amplitude (E_{THz}). As seen in this figure, the films with single orientation (i.e., film-A, film-G, and film-H) have almost the same E_{THz} amplitude regardless of their different crystalline structures. However, this amplitude is smaller than that of the films with coexisting structures (film-C, film-E, and film-F). To understand the variations in E_{THz} for various films, its correlation with structure and leakage current was explored. Figures 2(a) and 2(b) show the E_{THz} dependence on structural phase fraction and the x-ray diffraction (XRD) pattern around (001) peak, respectively, for various BFO/LSAT films. The left panel of Fig. 2(c) shows the E_{THz} dependence on the structural phase ratio[9] (i.e., ratio of the small phase to the large phase) and the right panel of this figure shows the leakage current dependence on the structural phase ratio. Also, the structural and other quantitative details of all the films are listed in Table I. It is clear in Fig. 2(c) that the films with coexisting phases have larger leakage current. Also, these films would have a larger density of defects owing to the structural defect and misfit dislocation that are inherent to coexisting structures.

Notably, film-C and film-F display the largest E_{THz} values, which is surprising in the sense that one would expect a decrease in E_{THz} amplitude for film-C and film-F due to their large density of misfit dislocations and defects. We further note that, among the films with coexisting structures, film-C and film-F display larger E_{THz} as compared to the E_{THz} of film-D. Correlating these terahertz-emission characteristic with their structure, we find that film-C and film-F possess only a small fraction of the secondary phase, while film-D has both phases of comparable amplitude. Also, Fig. 2(c) and

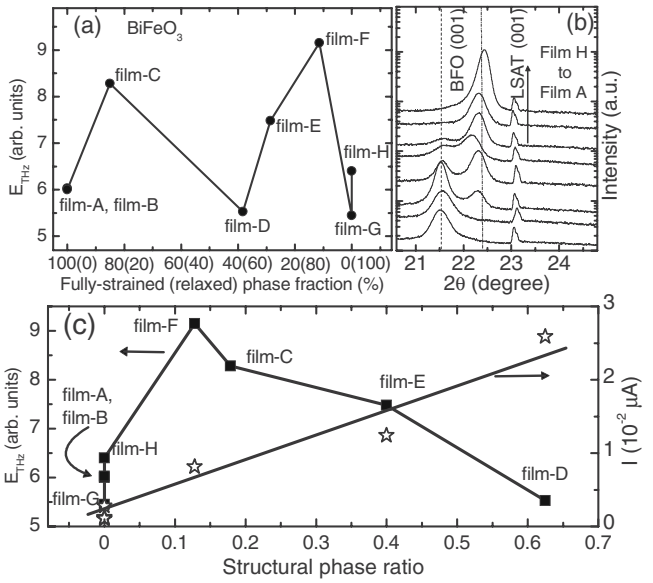

FIG. 2. (a) Peak terahertz amplitude as a function of structural phase fraction (fully strained/relaxed). (b) XRD pattern around (001) peak for all the films; the dashed vertical lines indicate the BFO peaks [peaks at lower and higher 2θ angles represent the strained phase and the (partially) relaxed phase, respectively]. (c) The left panel shows peak terahertz amplitude versus the structural phase ratio (small phase to large phase), while the right panel shows respective leakage current of various films; the solid line is a guide for the eye. It should be noted that nearly the same leakage current for films-A, B, G, and H might not enable us to clearly distinguish their data points.

Table I depict that a very low leakage current for film-A, film-B, and film-H increases optimally for film-C, film-E,

TABLE I. Structure, peak terahertz-emission amplitude (E_{THz}), leakage current, and structural phase ratio of various $BiFeO_3$ thin films.

Sample (thickness)	Structure	E_{THz} (arb. units)	Leakage current (μA)	Structural phase ratio
Film-A (65 nm)	Fully strained	6.03	0.1×10^{-2}	100
Film-B (75 nm)	Fully strained	6.00	0.1×10^{-2}	100
Film-C (85 nm)	Mixed	8.28		85
Film-D (95 nm)	Mixed	5.53	2.6×10^{-2}	38
Film-E (110 nm)	Mixed	7.48	1.2×10^{-2}	28
Film-F (110 nm)	Mixed	9.15	0.8×10^{-2}	11
Film-G (110 nm)	Partially relaxed	5.48	0.3×10^{-2}	0
Film-H (200 nm)	Partially relaxed	6.40	0.3×10^{-2}	0

and film-F, and then increases significantly for film-D. The largest E_{THz} amplitude manifests for the films with optimal leakage current. These data help us surmise that only a small fraction of the secondary phase or the low or optimal leakage current (as is the case of film-C and film-F) is conducive for improving the terahertz-emission efficiency and that the further increase in leakage current (as is the case of film-D) is detrimental for terahertz emission.

In semiconductors and strongly correlated materials, the illumination by laser pulses generates a current surge. The lifetime of carriers in this current surge is of the order of picoseconds, and carriers emit electromagnetic radiation at the far field in the terahertz frequency range according to the principle of classical electrodynamics[2] as

$$E_{\mathrm{THz}} \propto \frac{\partial J}{\partial t}, \tag{1}$$

where E_{THz} is the electric field of terahertz radiation at far field, and J is the current density. Now, according to Eq. (1), the terahertz emission from a ferroelectric material may be understood as follows. An ideal electric polarized state (P) consists of only bound immobile charges, as may be the case for ferroelectric $BiFeO_3$. Upon illumination by femtosecond laser pulses, these bound charges (carriers) become temporally mobile with a lifetime in the range of picoseconds before being trapped in the bound state of polarization potential. This current surge potentially denotes the temporal change of current density (J) in the picosecond time scale, which accounts for the generation of terahertz radiation at far field on the basis of Eq. (1). Using Ohm's law $J=\sigma E_{\mathrm{eff}}$ and the relation $\sigma=en_{\mu}$, where E_{eff}, e, n, and μ are the effective electric field that acts on the charge carriers, the elementary charge, the carrier density, and the carrier mobility, respectively, Eq. (1) can be modified as

$$E_{\mathrm{THz}} \propto \frac{\partial}{\partial t}(en\mu E_{eff}) \propto e\mu\left(E_{eff}\frac{\partial n}{\partial t} + n\frac{\partial E e_{ff}}{\partial t}\right). \tag{2}$$

After laser illumination, i.e., the state immediately after carrier excitation, only the first term on the right-hand side of Eq. (2) would be effective for terahertz radiation. The second term expresses the ultrafast screening of E_{eff} by the photogenerated carriers. This term has negative contribution to the terahertz emission when a large laser power (used for illumination) and/or a large applied bias result in a large density of photogenerated carriers that are effective in screening the E_{eff}. In the present study, we have compared the terahertz emission obtained in zero applied bias and a low laser power of ~10 mW. Hence, the impact of the second term of Eq. (2) would be insignificant and can be neglected. Thus, only the first term on the right-hand side of Eq. (2) accounts for terahertz emission. Defining the carrier density before and after laser illumination as n_{leak} and n_{photo}, respectively, Eq. (2) can be modified roughly as

$$E_{\mathrm{THz}} \propto e\mu E_{eff}\frac{\partial n}{\partial t} \propto e\mu E_{eff}(n_{photo}+n_{leak}) - e\mu E_{eff}n_{leak}$$
$$\propto e\mu E_{eff}n_{photo}. \tag{3}$$

Here, it is noticed that n_{leak} (that arises from the leakage current) does not show any direct contribution to the emission of terahertz radiation. However, in an indirect way, the presence of large n_{leak} would hinder the saturation of polarized state and influence the E_{THz}. More elaborately, in BFO/LSAT films with coexisting structures (from film-C to film-F), the variations in E_{THz} can be explained to originate from a combination of two factors—the structural defects and the leakage current, as follows.

(i) Structural defects. In mixed-phase films, the inherent defects and dislocations may act as trapping centers for the carriers. This would decrease the mean free path of carriers of the photogenerated current pulse. As the reduction in the mean free path of carriers increases terahertz-emission amplitude,[2] the films with mixed phase will exhibit larger terahertz amplitude.

(ii) Leakage current. The E_{THz} can be affected by the amplitude of leakage current. A large leakage current will certainly reduce E_{THz} as it will not enable the applied electric field to achieve the saturation polarization. For instance, film-D has the largest leakage current and the least E_{THz} amongst the films with coexisting structures (from film-C to film-F). In this film, the applied electric field would partially dissipate in leakage current which, resultantly, would render the effective electric field insufficient to achieve saturation polarization. Here, it should be noted that the terahertz emission is achieved in the polarized state. Therefore, in the case of film-D, unsaturated polarization prior to illumination is a dominant factor for low E_{THz}. Now, we consider the probable effect of low (or optimal) leakage current, as is the case for other mixed-phase films (films-E and film-F). In these films, the leakage current is not sufficient to prevent achieving a near saturation in polarization. Thus, the low (or optimal) leakage current in mixed-phase films will have nearly no effect on terahertz emission. Therefore, as mentioned in the previous section, the mixed-phase films with low leakage current will have their emission efficiency enhanced only as a result of larger defect density.

At this point of discussions, it may be recalled that the fully strained films (film-A and film-B) and the relaxed films (film-G and film-H) exhibit nearly the same E_{THz}. This is an indication that the ferroelectric polarization in BFO/LSAT films is not likely to be influenced by epitaxial strain, which is consistent with the theoretical predictions made by Ederer and Spaldin[10] for $BiFeO_3$. However, it should be noted that this effect is a characteristic of only $BiFeO_3$, whereas some other ferroelectrics such as $BaTiO_3$ and $PbTiO_3$ are known to exhibit a strain dependent ferroelectric polarization.[10] Also, to authenticate all above-mentioned discussions on the structural dependence of terahertz emission, it is imperative to consider the effect of the amount of material (which would vary with thickness of the film) on terahertz emission. A thickness range of 65–200 nm of the presently studied BFO/LSAT films seems to have no apparent impact of material thickness on terahertz-emission efficiency. This is evident from only a small difference in E_{THz} values of 110 nm film (film-G) and 200 nm film (film-H), both of which have the same structure. This further suggests that the range of thickness (65–200 nm) of the BFO/LSAT films is not wide enough to have considerable impact on laser photon absorption and the resultant terahertz emission.

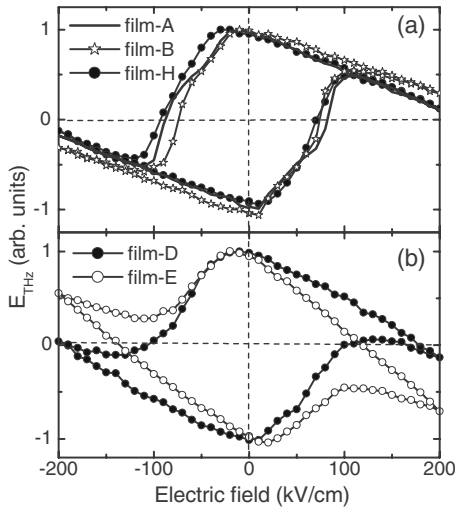

FIG. 3. The electric field (E) versus peak terahertz-amplitude (E_{THz}) hysteresis loops (a) for film-A, film-B, and film-H, and (b) for film-D and film-E. The sample was first poled in an electric field of −200 kV/cm, and then the data were collected in the electric-field sequence of 0 kV/cm→200 kV/cm→0 kV/cm →−200 kV/cm→0 kV/cm.

To obtain further insight into the terahertz-emission properties and to evaluate the ferroelectric properties of BFO/LSAT films, electric-field (E) dependence of the E_{THz} was measured for all the films. This generates an E_{THz}-E hysteresis loop that directly reflects the ferroelectric properties of the films.[11] Figure 3 shows the E_{THz}-E loops for (a) film-A, film-B, and film-H, which are representative of the films with single structure, and (b) for film-D and film-E, which are representative of the films with coexisting structures. A dominant feature of E_{THz}-E loops which is different from the conventional ferroelectric hysteresis loops is the tilting of E_{THz}-E loops toward the electric-field axis. This can be explained by considering the screening of photogenerated carriers by the electric field biased to a pair of electrodes, as described in Ref. 5. We observe some distinctive features in these loops, namely, (i) film-A, film-B, and film-H possess the same degree of tilt and the same coercivity of ~70 kV/cm, irrespective of their different structures. These loops completely close at an electric field of around ~110 kV/cm, which resembles the characteristic of a saturated ferroelectric hysteresis loop, and (ii) the loops of film-D and film-E have a larger degree of tilt and do not completely saturate. These variations in E_{THz}-E loops may be understood by invoking their correlation with the structure and the terahertz-emission efficiency. The films with single structure, analogous to their similar E_{THz}, possess almost similar E_{THz}-E hysteretic properties—saturated loops with the same optimal tilt. Comparatively, the films with coexisting structures display unsaturated E_{THz}-E with a larger degree of tilt toward the electric-field axis, which can be explained in terms of their leakage current characteristic [Fig. 2(c)]. For instance, a considerably large tilt of loop for film-D is consistent with its large leakage current and so is for film-E. As stated before, the partial dissipation of the E_{eff} in leakage current causes incomplete polarization and this will result in largely tilted unsaturated hysteresis loops. Alternatively, it may be contemplated that the optical dose is not enough to assist the electric field to achieve complete polarization.

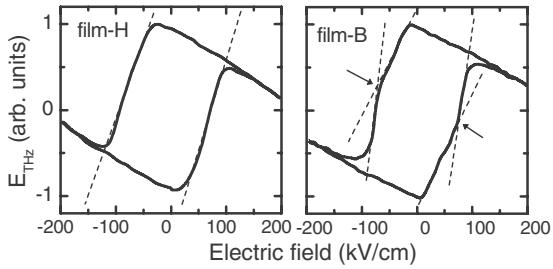

FIG. 4. The electric field (E) versus peak terahertz-amplitude (E_{THz}) hysteresis loops for film-H and film-B. A single dashed line in the hysteresis loop of film-H indicate one slope while transformation from $-E_{THz}$ to $+E_{THz}$, while two dashed lines in the hysteresis loop of film-B indicate that $-E_{THz}$ transforms to $+E_{THz}$ in two steps. The arrows indicate the change of slope.

Despite the above-mentioned similar features in E_{THz}-E loops of the relaxed films and the strained films, there is a pronounced difference in the shape of these loops. To illustrate this effect, the E_{THz}-E loops are plotted separately for the relaxed lattice (film-H) and the strained lattice (film-B) in Fig. 4. The electric-field dependent transformation from $-E_{THz}$ to $+E_{THz}$, or vice versa, in E_{THz}-E loop occurs in a smooth way for film-H. The same transformation occurs in a different way for film-A; the E_{THz} increases at one rate from 10 to 70 kV/cm and at another rate from 70 to 100 kV/cm. A similar transition occurs from −10 to −100 kV/cm. These different rates produce two slopes which are symmetric to their counterparts on opposite sides of the electric-field axis, as shown by dashed lines for film-B in Fig. 4. In ferroelectrics, a similar behavior of ferroelectric hysteretic loops has been suggested to arise from the aging effect when the arrangement of defects conforms to structural symmetry.[12] This, however, is not pertinent in the present case since our films were not subjected to the aging effect. In such a case, it is obvious to assume this behavior as intrinsic to the structure and associate it with their respective fully strained and relaxed lattices. Though it is not possible to exactly identify the nature of lattice contribution from the present data, a conjecture with some theoretical predictions of lattice effects in $BiFeO_3$ might enhance our understanding of these results.[10,13] In $BiFeO_3$, the spontaneous electric polarization and the axis of antiferromagnetic ordering are directed along the (111) direction. It has been predicted theoretically that there exists a sixfold degeneracy of the orientation of the antiferromagnetic sublattice within the (111) plane.[10,13] It is further noted that the sixfold degeneracy of the magnetization sublattice can be lifted by inducing the monoclinic distortion (by the means of strained films) in its rhombohedral structure, which might induce alterations in strain induced coupling of ferroelectric polarization and antiferromagnetic axis.[10] As a result, the switching process of ferroelectric polarization of a fully strained lattice would be different than that of the relaxed rhombohedral lattice. The 65 and 75 nm BFO/LSAT thin films, in the present case, are a sure case of

coherently strained structure. Therefore, the polarization switching process of these films is different than that of the partially relaxed 200 nm BFO/LSAT film (Fig. 4). However, further investigations with additional characterizations might be useful to reach a clear understanding of this structural contribution, and is left for the future.

In summary, the terahertz-emission as a function of structure from $BiFeO_3$ films on $(LaAlO_3)_{0.3}(Sr_2AlTaO_6)_{0.7}$ (0 0 1) substrate reveals that terahertz-emission efficiency in the absence of applied bias is nearly independent of the lattice, but depends on the quality of films. On the other hand, the electric-field dependent terahertz-emission hysteresis loops possess lattice dependent characteristics. These loops facilitating an indirect evaluation of ferroelectric properties of BFO/LSAT films depict that the ferroelectric polarization switching is lattice dependent, while the coercivity has no impact on the structural lattice.

This work was supported in part by "Nanotechnology Support Project" of the Ministry of Education, Culture, Sports, Science and Technology (MEXT), Japan. D.S.R. thanks JSPS for the financial support.

*rana-d@ile.osaka-u.ac.jp
†tonouchi@ile.osaka-u.ac.jp

[1] M. Tonouchi, Nat. Photonics **1**, 97 (2007).
[2] N. Kida, H. Murakami, and M. Tonouchi, in *Terahertz Optoelectronics*, edited by K. Sakai (Springer-Verlag, Berlin, 2005), p. 271.
[3] N. A. Hill, J. Phys. Chem. B **104**, 6694 (2000).
[4] W. Eerenstein, N. D. Mathur, and J. F. Scott, Nature (London) **442**, 759 (2006).
[5] K. Takahashi, N. Kida, and M. Tonouchi, Phys. Rev. Lett. **96**, 117402 (2006).
[6] K. Takahashi and M. Tonouchi, Jpn. J. Appl. Phys., Part 2 **45**, L755 (2006).
[7] K. Takahashi and M. Tonouchi, Appl. Phys. Lett. **90**, 052908 (2007).
[8] D. S. Rana, K. Takahashi, K. R. Mavani, I. Kawayama, H. Murakami, M. Tonouchi, T. Yanagida, H. Tanaka, and T. Kawai, Phys. Rev. B **75**, 060405(R) (2007).
[9] Given the fact that full widths at half maximum of the XRD peaks of coexisting phases are nearly same, the structural phase ratio was determined by the ratio of the height of XRD peaks of two coexisting phases, i.e., the ratio of the height of XRD peak of the minor structural phase to that of the major structural phase. For instance, in film-D, a minor phase of ~40% (fully strained) and major phase of ~60% (partially relaxed) will yield a structural phase ratio of ~0.66. Similarly, in film-C, a minor phase of ~14% (partially relaxed) and a major phase of ~86% (fully strained) will yield a structural phase ratio of ~0.16.
[10] C. Ederer and N. A. Spaldin, Phys. Rev. B **71**, 060401(R) (2005); Phys. Rev. Lett. **95**, 257601 (2005).
[11] The positive and negative polarities of E_{THz} (as seen in E_{THz}-E hysteresis loop) arise from the change in polarity of the applied bias. Terahertz radiation is emitted when photogenerated carriers are accelerated by the applied bias. Changing the polarity of the applied bias reverses the direction of acceleration of carriers and, hence, the polarity of resultant terahertz emission with respect to that of the probe pulse. The positive and negative E_{THz} in E_{THz}-E hysteresis loop imply that the orientation of electric dipoles or the ferroelectric domains differ by 180° or, in other words, ferroelectric domains with opposite polarities as switched by applied electric field.
[12] L. X. Zhang and X. Ren, Phys. Rev. B **73**, 094121 (2006).
[13] R. Ramesh and N. A. Spaldin, Nat. Mater. **6**, 21 (2006).